Electronic supplementary materials *Mendeleev Commun.*, 2022, **32**, 645–648

Tracking nitrogen-to-nickel ratio and prevalent paramagnetic species in synthetic diamonds by electron spin resonance at 90 K

Vladimir Yu. Osipov, Fedor M. Shakhov, Nikolai M. Romanov and Kazuyuki Takai

Contents

S1. Synthesis of diamond microcrystals

Microcrystals of diamonds of the first type (MD1) were obtained as a result of rapid processing of a specially prepared graphite–nickel mixture at a temperature of 1650 °C and a pressure of 5 GPa. A schematic of a high-pressure cell used for the synthesis of diamond microcrystals can be found in Ref. S1. Details and features of the growth of such microcrystals at high pressure and high temperature can be found in Ref. S2. The main operations used in this synthesis are as follows. The mixture was prepared from graphite powder of > 99.5% purity with a particle size of 315-400 microns and metallic nickel powder with a particle size of up to 71 microns, taken in a proportion of 50 wt%: 50 wt%. Nickel melts at a temperature of 1650 °C and a pressure of 5 GPa and dissolves the carbon in it. The indicated temperature and pressure correspond to the condition of diamond nucleation and the growth of diamond crystals from carbon dissolved in nickel. Microcrystals of the second type (MD2) were obtained by adding to the pre-prepared graphite-nickel (50 wt%: 50 wt%) charge about 10 wt% powdered aluminum (particle size up to 140 microns) to obtain a mixture of C–Ni–Al with a composition of 45.5 : 45.5 : 9. The diamond phase yield from graphite was, respectively, about 31% and 18% for the synthesized samples of the first and second types. Both samples contain nickel and nitrogen, but the nitrogen content in the second sample is much lower due to the binding of a part of nitrogen by aluminum in the molten metal of the carbon-nickel charge. In both cases, the synthesized crystals were from 30 to 160 microns in size. Electron microscopic images of the obtained crystallites are shown in Figure S1. They were obtained using a scanning electron microscope JEOL JSM-6390 (Japan). It can be seen that microcrystals of both types have an arbitrary uncut shape with a coarse roughness, and only a small part of the crystallites exhibits complete or partial faceting (Figure S1(*d*)). Despite the unfaceted arbitrary shape of most MD2 microcrystals (Figure S1(*c*)), they have a sufficiently high quality of the crystal lattice and a relatively low (~133 ppm) concentration of paramagnetic defects. This is evidenced by studies of microdiamonds by the method of electron paramagnetic resonance (EPR).

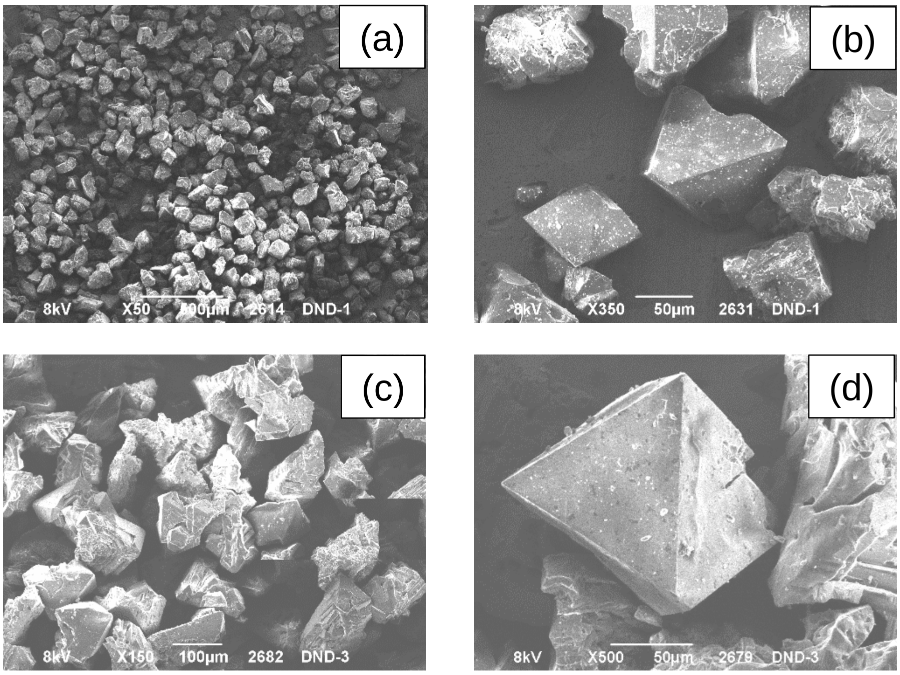

Figure S1. Scanning electron microscopy images of microcrystals MD1 (a,b) and MD2 (c, d). Bars, µm: a - 500, b - 50, c - 100, d - 50. Microcrystals of octahedral shape are clearly seen in panels (b) and (d).

Energy Dispersive X-Ray (EDX) analysis was carried out using the same scanning electron microscope equipped with an attached EDX spectroscope (analyzer) Oxford Instruments INCA x-act (UK). Elemental composition information was obtained by analyzing the diamond powder surface on a conductive substrate. Thorough analysis did not show the presence of nitrogen and nickel in the material, which did not exclude its possible presence in the material at a level below the sensitivity threshold of the SEM-EDX method (0.1-0.2 at%).

S2. Characterization

Electron paramagnetic resonance

The EPR spectra of the samples were studied at Hosei University (Japan). They were recorded at room temperature or at low temperature (T=90 K) using an EPR spectrometer (JES-FA 300, JEOL, Japan) at a microwave frequency of 9.070 GHz. A powder weighing 10–12 mg was first poured into a thin glass capillary tube up to 25 mm long, which was sealed at both ends, and then the latter was placed at the bottom of a long EPR quartz tube with an outer diameter of 5 mm. The open end of the long EPR tube was sealed against moisture. EPR spectra of signals with *g*-factors g ≈ 2 were recorded in the interval from 308 to 339 mT, with microwave power of P_{MW} = 0.003 mW, magnetic field modulation amplitude A_m = 0.03 mT and frequency ν = 100 kHz, amplifier gain *G* = 500 (or less), and *N*=10 (or 8) signal accumulation cycles. The time constant was 0.03 s, and the total recording time for the magnetic field sweep over the 308 to 339 mT interval was 60 s. These parameters were chosen to obtain the optimal signal-to-noise ratio. The spectra were saved with the number of points along the magnetic field axis equal to 8192. Due to the fact that a low-temperature cryostat was used to ensure low-temperature measurements at

T=90 K and there was no space between the electromagnet poles for attaching additional sensors, the refinement and correction of the magnetic field values using NMR magnetometer was not produced. The magnetic field was measured with a standard Hall sensor glued to one of the poles of an electromagnet. Note that in all presented EPR spectra the horizontal axis shows the uncorrected value of the magnetic field obtained from the Hall sensor, and for precision calculations, the field was corrected by several G downward when using a powder EPR standard with a *g*-factor of 2.0024.

EPR spectra taken at 90 K showed the presence of nickel impurities in the -1 charge state in the diamond lattice in addition to the basic nitrogen impurities in the material. Well-identified signatures from the EPR signals of nickel and nitrogen are contained in the spectra of both samples MD1 and MD2. All lines in the EPR spectrum of sample MD1 are broadened due to the high concentration of both paramagnetic nitrogen, the main broadening agent in the system and other *spin-half* paramagnetic species having the same *g*-factor. This implies the dipole-dipole mechanism of line broadening from paramagnetic spins. In this case, the signal from nickel in sample MD1 is also broadened at 90 K.

Schematics of the microwave transitions responsible for the absorption of microwaves in nickel (Ni_S^-) and nitrogen impurities are shown in Figure S2. These schemes are well known. However, we emphasize that in the case of nickel in the Ni_S^- state, all three microwave transitions 1,2 and 3 (shown in the upper part of Figure S2) are responsible for the formation of a single EPR line with a *g*-factor of 2.0319.

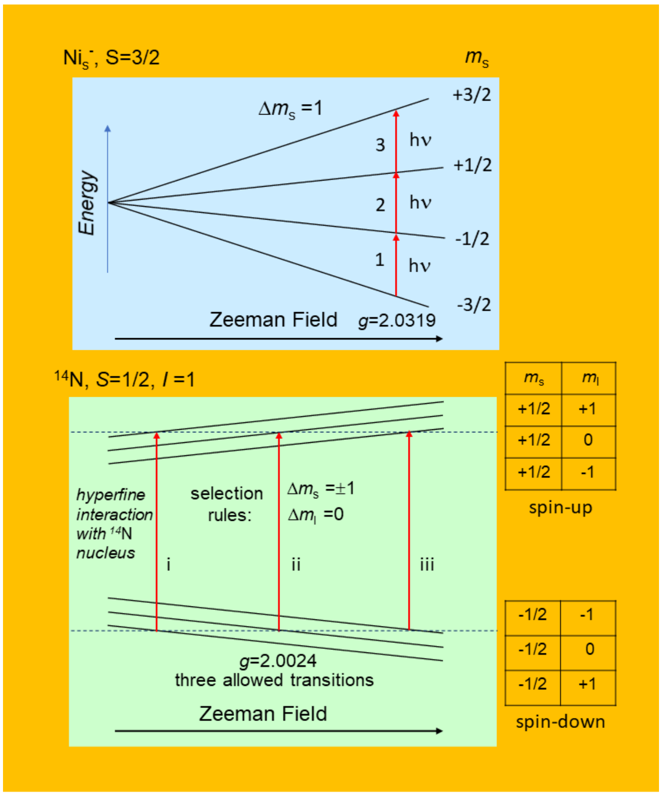

Figure S2. Schematics of the microwave transitions responsible for the absorption of microwaves in nickel Ni_S^- (top part) and nitrogen N_S^0(bottom part) impurities in diamond. m_S- magnetic spin quantum number, m_I – magnetic nuclear quantum number. Red arrows – allowed microwave transitions Δm_S=1.

In turn, for the MD2 sample grown using a nitrogen getter, all characteristic lines (as for impurity nitrogen and nickel) in the EPR spectrum taken at 90 K are relatively narrow. This suggests a low concentration of paramagnetic nitrogen in such a material and the effectiveness of aluminum as a nitrogen getter (or even nitrogen separator preventing its penetration to the growing diamond nucleus) for this type of synthesis.

S3. Aluminum as nitrogen and nickel getter/separator

The addition of aluminum to the nickel–graphite mixture leads to the fact that the concentration of nitrogen and nickel in the synthesized diamond microcrystals drops by about 3 times. The source of impurity nitrogen entering the microcrystals is the molecular nitrogen of air, which is present in the initial charge due to its sorption by graphite powder. In the process of high-temperature synthesis at high pressure, aluminum is approximately uniformly distributed over the entire volume of the catalyst melt, but its concentration is increased near the crystalline faces of growing diamond nuclei. This layer with an increased concentration of aluminum binds nitrogen and prevents it from entering the growing microcrystal. The layer enriched with aluminum has the same effect on nickel, preventing its penetration into microcrystals in large quantities. Thus, we can consider the layer enriched with aluminum as a nickel separator, since the concentration of the latter in microcrystals is reduced by the same number of times as for nitrogen. Figure S3 shows the corresponding model of the action of the aluminum-rich layer.

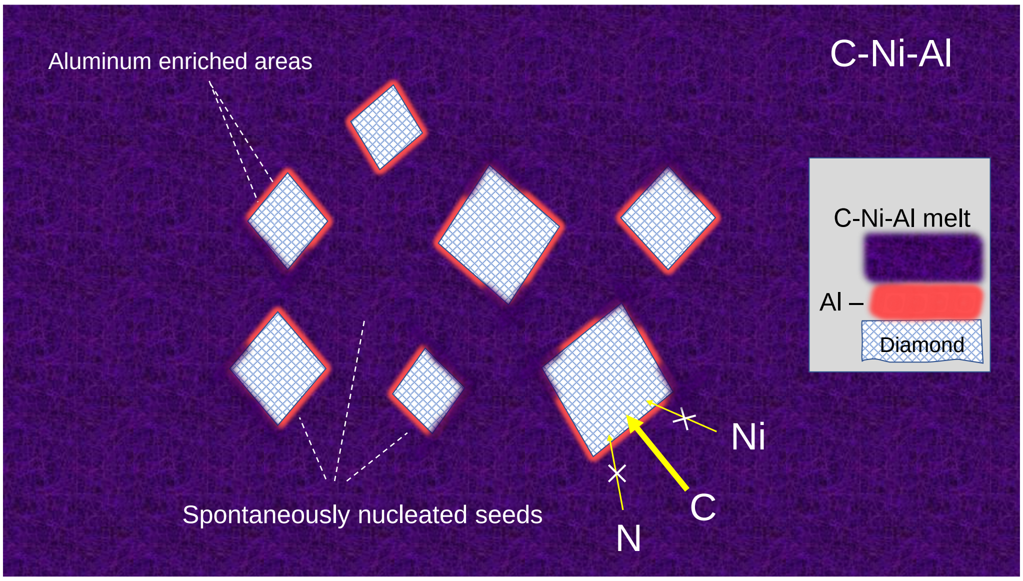

Figure S3. Scheme of the formation of diamond nuclei-crystallites and areas with a high content of aluminum (filled in red) for a small arbitrary section of C–Ni–Al charge with carbon dissolved in the nickel melt. (Graphite particles are not shown in the figure).

References

[S1] F.M. Shakhov, A.M. Abyzov, and K. Takai, *J. Solid State Chem.*, 2017, **256**, 72.
[S2] F.M. Shakhov, V.Yu. Osipov, A.A. Krasilin, K. Iizuka and R. Oshima, *J. Solid State Chem.*, 2022, **307**, 122804.